THE JOURNAL OF PHYSICAL CHEMISTRY B

Article

pubs.acs.org/JPCB

How Quickly Can a β-Hairpin Fold from Its Transition State?

Beatrice N. Markiewicz,[†] Lijiang Yang,[§,∥] Robert M. Culik,[‡] Yi Qin Gao,*[,§,∥] and Feng Gai*[,†]

[†]Department of Chemistry and [‡]Department of Biochemistry and Biophysics, University of Pennsylvania, Philadelphia, Pennsylvania 19104, United States

[§]Beijing National Laboratory for Molecular Sciences, College of Chemistry and Molecular Engineering, and [∥]Biodynamic Optical Imaging Center, Peking University, Beijing, 100871, China

Supporting Information

ABSTRACT: Understanding the structural nature of the free energy bottleneck(s) encountered in protein folding is essential to elucidating the underlying dynamics and mechanism. For this reason, several techniques, including Φ-value analysis, have previously been developed to infer the structural characteristics of such high free-energy or transition states. Herein we propose that one (or few) appropriately placed backbone and/or side chain cross-linkers, such as disulfides, could be used to populate a thermodynamically accessible conformational state that mimics the folding transition state. Specifically, we test this hypothesis on a model β-hairpin, Trpzip4, as its folding mechanism has been extensively studied and is well understood. Our results show that cross-linking the two β-strands near the turn region increases the folding rate by an order of magnitude, to about $(500\ \text{ns})^{-1}$, whereas cross-linking the termini results in a hyperstable β-hairpin that has essentially the same folding rate as the uncross-linked peptide. Taken together, these findings suggest that cross-linking is not only a useful strategy to manipulate folding free energy barriers, as shown in other studies, but also, in some cases, it can be used to stabilize a folding transition state analogue and allow for direct assessment of the folding process on the downhill side of the free energy barrier. The calculated free energy landscape of the cross-linked Trpzip4 also supports this picture. An empirical analysis further suggests, when folding of β-hairpins does not involve a significant free energy barrier, the folding time (τ) follows a power law dependence on the number of hydrogen bonds to be formed (n_H), namely, $\tau = \tau_0 n_H^{\alpha}$, with $\tau_0 = 20$ ns and $\alpha = 2.3$.

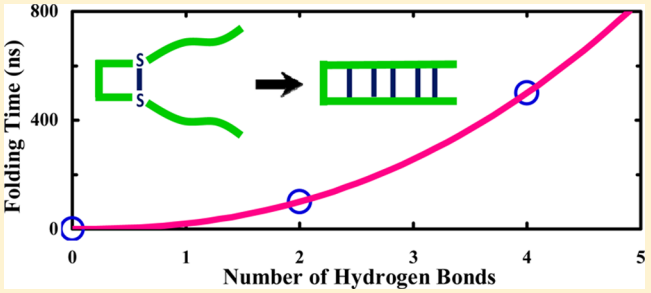

INTRODUCTION

Protein folding occurs spontaneously, as the process lowers the free energy of the system upon formation of the folded state. During folding, however, the entropic loss can transiently outweigh the enthalpic gain, thus resulting in one or more free energy bottlenecks or transition states along a given folding pathway.[1−3] Because, for a given protein, identifying the structure of the folding transition state(s) is key to elucidating its folding mechanism, these high energy states have been the subject of many previous studies.[4] Due to the transient nature of these states, however, it is extremely difficult, if not impossible, to directly observe and study them experimentally. As such, only indirect methods[5−8] have been used to yield structural information about folding transition states. For example, one such method, Φ-value analysis, uses site-specific side chain mutations in conjunction with stability and kinetics measurements to infer if a certain side chain becomes native-like at the transition state.[9−11] While these methods have proven invaluable in the study and understanding of how proteins fold, they cannot be used to isolate the folding transition state of interest for further structural and dynamic investigations. Thus, it would be very useful to devise a method that can convert a folding transition state to a thermodynamically stable and accessible state. Herein, we propose, based on the transition state analog (TSA) methodology commonly used in mechanistic studies of enzymatic reactions,[12,13] that it is possible, at least for small protein systems, to use cross-linking strategies to accomplish this goal.

In enzymatic studies, the TSA represents a stable, non-reactive enzyme−substrate complex that mimics the transition state of the reaction of interest.[14,15] In such biochemical reactions, the transition state is an ensemble of high energy configurations near a saddle point along the free energy coordinate that is experimentally inaccessible. However, since the TSA is thermodynamically accessible and also captures strongly bound interactions that translate to a transition state-like complex,[16] it allows for a more detailed structural characterization of the transition state, which is otherwise difficult to achieve.[17] For protein folding, another advantage of being able to engineer TSAs is that, besides what is mentioned above, it would enable us to measure folding dynamics that are otherwise inaccessible, i.e., the conformational dynamics at the downhill side of the folding free energy barrier. For small and two-state folding proteins, the folding transition state often

Received: January 22, 2014
Revised: March 3, 2014
Published: March 10, 2014

   dx.doi.org/10.1021/jp500774q | J. Phys. Chem. B 2014, 118, 3317−3325

consists of a relatively small number of key side chain-side chain and backbone−backbone hydrogen bond interactions. Thus, a viable strategy that could be used to create a folding TSA is to cross-link some of these key interactions via covalent bonds, to lower the entropic cost of forming the transition state. To test the feasibility of this idea, herein we apply it to one of the simplest folding systems, the β-hairpin.

Since the folded structure of β-hairpins consists of a series of backbone−backbone hydrogen bonds, some of which exist in the transition state,[18−25] an ideal approach to create a folding TSA would be to covalently cross-link one or multiple of these hydrogen bonds. Converting a backbone−backbone hydrogen bond to a chemical bond without introducing significant structural perturbations, however, is challenging. Thus, instead we seek to use a side chain disulfide cross-linker to help, albeit in an indirect manner, restrain a particular native backbone−backbone hydrogen bond that is predicted to form in the transition state. A disulfide bond may introduce strain to these hydrogen bonded sites, however, experiments on a small model system have shown that the favorable enthalpic contribution of the cross-linker could compensate for this potential geometric distortion.[26] While the strategy of cross-linking has been widely used to increase protein stability,[26−31] trigger protein unfolding,[32,33] and to interrogate, in the context of Φ-value analysis,[34−38] folding mechanisms, to the best of our knowledge it has not been used to create a thermodynamically stable conformation that structurally resembles the folding transition state. As many studies have shown, the major folding pathway of Trpzip β-hairpins[39−51] involves a transition state wherein the turn structure is at least partially formed. Thus, we propose, using Trpzip4 as a testbed, to create a β-hairpin folding TSA by forcing the formation of a backbone−backbone hydrogen bond critical to the stability of the β-turn between Asp6 and Thr11 (Table 1). As indicated (Figure 1), such a conformational constraint on a system that folds cooperatively, if effective, is expected to divide the unfolded state ensemble into two structurally distinguishable subpopulations: one with a native or native-like turn (U_A), whereas the other is completely unstructured (U_B). If U_A behaves like a folding TSA, we expect that its folding rate will be significantly increased with respect to the wild-type. On the other hand, the folding kinetics of U_B are expected to be similar to those of the wild-type because both pathways (i.e., $U_B \rightarrow F$ and $U_B \rightarrow U_A \rightarrow F$) involve the formation of the turn, the rate limiting step in Trpzip4 folding.[44] Indeed, consistent with this picture, our results show that the conformational relaxation kinetics of this cross-linked Trpzip4 variant, induced by a rapid temperature-jump (T-jump) and measured via time-resolved infrared (IR) spectroscopy,[52] are biphasic, with one phase having a relaxation rate that is almost identical to that of the wild-type and another relaxing an order of magnitude faster. Further evidence supporting our hypothesis (Figure 1) is that T-jump measurements on another cross-linked Trpzip variant, whose two ends are connected via a disulfide (Table 1), only show single-exponential relaxation kinetics, as are observed for the wild-type, but with a slower relaxation rate, due mainly to a decrease in the unfolding rate.

Table 1. Name and Sequence of the Peptides Used in the Current Study[a]

peptide	sequence
Trpzip4	GEWTWDDATKTWTWTE
TZ4-T-CL	GEWTW**C**DATK**C**WTWTE
TZ4-T-UL	GEWTWCDATKCWTWTE
TZ4-E-CL	**C**EWTWDDATKTWTWT**C**
TZ4-E-UL	CEWTWDDATKTWTWTC

[a]Underlines indicate disulfide cross-linking.

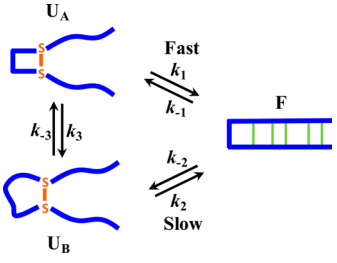

Figure 1. Cartoon representation of the proposed folding mechanism wherein two distinguishable unfolded states, U_A and U_B, are populated, due to the disulfide cross-linker in the turn region.

MATERIALS AND METHODS

All peptides were synthesized using standard 9-fluorenylmethoxy-carbonyl (Fmoc) methods on a PS3 peptide synthesizer (Protein Technologies, Woburn, MA) and purified by reverse-phase high-performance liquid chromatography (HPLC). Amino acids were purchased from Advanced ChemTech (Louisville, KY). MALDI-TOF mass spectrometry was used to characterize the identity of the synthesized peptides. Disulfide formation was accomplished, using a published protocol,[53] via dimethyl sulfoxide (DMSO). Specifically, an appropriate amount of pure peptide solid was dissolved in a 20% DMSO solution in H_2O, and the resulting mixture was stirred for 4 h at room temperature, allowing the oxidation reaction to complete. Subsequently, a second round of HPLC was carried out to purify the disulfide cross-linked peptide, and the identity was further verified by MALDI-TOF mass spectrometry. All peptide samples were prepared by directly dissolving the lyophilized peptide solid in D_2O and the final pH of the peptide samples was approximately 3. For the uncross-linked peptide samples, a reducing agent, tris(2-carboxyethyl)-phosphine hydrochloride (TCEP), was also added at a concentration of approximately 10 times that of the peptide, to ensure that disulfide bonds were completely removed. The peptide concentration was determined optically using the absorbance at 280 nm and ε_{280} = 22 125 cm^{-1} M^{-1}, and, for all peptide samples, residual trifluoroacetic acid (TFA) from peptide cleavage has been removed via deuterium chloride (DCl) exchange.

Static and Time-Resolved Spectroscopic Measurements. The instruments and conditions used to collect the spectroscopic data, including static circular dichroism (CD) and infrared (IR) and time-resolved IR measurements, are identical to those used previously.[54] For the IR measurements, the peptide concentration was approximately 2 mM, prepared in D_2O (pH 3). The probing frequency in the T-jump experiment was 1626 cm^{-1}, and the T-jump amplitude was in the range of 8−12 °C.

Molecular Dynamics Simulations Using Integrated Tempering Enhanced Sampling. Molecular dynamics (MD) simulations were performed for wild-type and cross-linked Trpzip4 using the AMBER 11 package. The peptides were modeled with the AMBER FF96[55] all-atom force field, and the solvent was modeled with the GB^{OBC}/SA implicit

dx.doi.org/10.1021/jp500774q | J. Phys. Chem. B 2014, 118, 3317−3325

solvent model.[56] The salt concentration was set to 0.2 M, and the default surface tension was 5×10^{-3} kcal/mol/Å^2. The SHAKE[57] algorithm with a relative geometric tolerance of 10^{-5} was used to constrain all chemical bonds. Nonbonded cutoffs were not used in the simulations. For both wild-type and cross-linked Trpzip4, 10 independent trajectories were carried out for 200 ns (2 μs in total). In each trajectory, the fully extended structure of the polypeptide was first subjected to 2500 steps of minimization, and then the temperature of the system was established by velocity rearrangement from a Maxwell–Boltzmann distribution at 300 K. Afterward, the system was maintained at 300 K using the weak-coupling algorithm with a coupling constant of 0.5 ps^{-1}. The integrated tempering enhanced sampling (ITS)[58−60] method was used in the production run of each trajectory. In the present study, 100 temperatures, evenly distributed in the range of 270–470 K, were used in the ITS method to ensure the efficient sampling of the desired energy.

RESULTS AND DISCUSSION

We chose the Trpzip4 β-hairpin (Table 1) as our model system because of its small size and the large body of information on its folding mechanism.[42,44,61−66] The major folding pathway, as suggested by previous studies,[42,44] begins with turn formation, which is a thermodynamically unfavorable event and hence results in a folding free energy barrier, followed by the sequential creation of backbone–backbone hydrogen bonds further away from the turn in a 'zipping out' manner. Thus, based on this picture as well as the NMR structure,[67] which indicates that the first interstrand hydrogen bond is formed between the amides of Asp6 and Thr11, we propose to use a disulfide to reduce the number of possible configurations available near these residues with the expectation that this restriction is sufficient to produce an unfolded species that has a native-like turn and, therefore, behaves like a folding TSA. To accomplish this, we first mutated Asp6 and Thr11 to cysteine, and then the resulting mutant was placed under oxidizing conditions to promote disulfide bond formation. In addition, we have studied another cross-linked variant of Trpzip4 with a disulfide formed at the peptide ends that serves as a control. For convenience, the sequences and abbreviations of all the peptides studied are summarized in Table 1.

Effect of Cross-Linking on the Thermal Stability of Trpzip4. As shown (Figure 2), the far-UV CD spectra of both cross-linked and uncross-linked peptides are in line with that of the wild-type,[44] exhibiting a positive band at 228 nm.[68] Since this CD feature signifies the $\pi-\pi^*$ exciton-coupling of the paired Trp residues in the folded state,[69−71] these results suggest that the mutations and disulfide constraints used in this study do not significantly perturb the native fold of Trpzip4. In addition, the chemical shifts obtained from the 1D ^{1}H NMR spectrum of TZ4-T-CL agree with previously published data,[67] and are well dispersed, which indicates a well-folded secondary structure (Figure S1, Supporting Information). As expected, CD thermal unfolding measurements indicate, for a given sequence, that cross-linking increases the thermal stability of the β-hairpin, in comparison to that of the uncross-linked peptide (Figure 3 and Table 2). Nevertheless, what is more interesting is that the T_m (~67 °C) of TZ4-T-CL is almost identical to that (~70 °C) of the wild-type,[42] indicating that the added disulfide constraint at this site does not significantly perturb β-hairpin stability, presumably because the enthalpic stabilization gained from the cross-linking is mostly offset by the conformational entropic loss in the unfolded state.[72] On the other hand, as observed in similar studies,[28,73] cross-linking the two ends of the Trpzip4 peptide results in a hyperstable β-hairpin with a T_m > 100 °C. This result is not surprising considering that the unfolding process, which, according to the zipping out folding mechanism, should 'unzip' the backbone–backbone hydrogen bonds of the hairpin starting from the strands' termini.

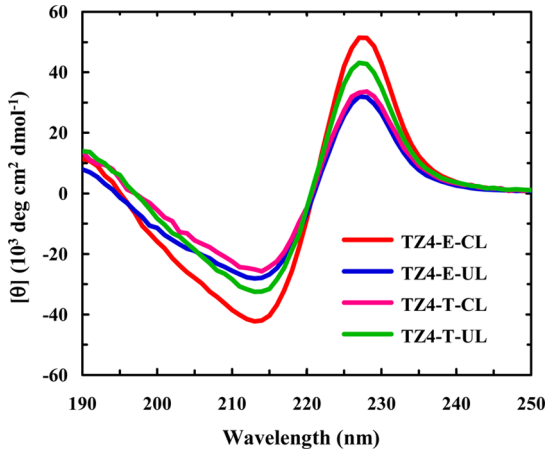

Figure 2. CD spectra of the cross-linked and uncross-linked Trpzip4 variants, as indicated.

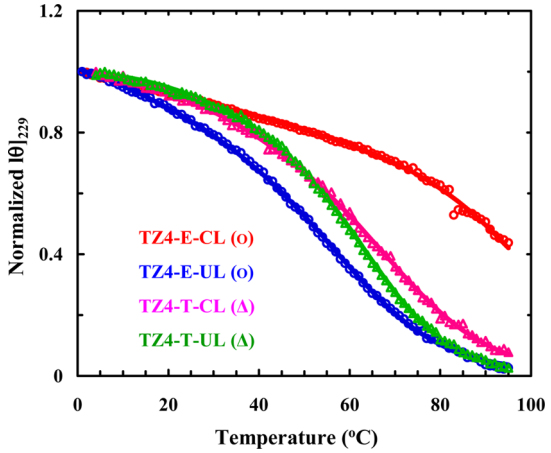

Figure 3. Normalized CD thermal unfolding curves of the cross-linked and uncross-linked Trpzip4 variants, as indicated. The solid lines are global fits of these data to a two-state model (Supporting Information) and the resultant thermodynamics parameters are listed in Table 2.

Effect of Mutation and Cross-Linking on the Relaxation Kinetics of Trpzip4. The conformational relaxation kinetics of these Trpzip4 variants were measured by a laser-induced T-jump IR technique, as was used in the study of the Trpzip4 wild-type peptide. As shown (Figure 4), unlike what was observed for the wild-type, the conformational relaxation of TZ4-T-CL, probed at 1626 cm^{-1}, proceeds with two distinct and well-separated kinetic phases, indicating that the disulfide cross-linking indeed, as proposed, changes the folding mechanism of Trpzip4, as the wild-type, in response to a T-jump, only shows single-exponential decays. Interestingly, as shown (Figure 5), the relaxation rate of the slow phase (τ_2) is almost identical to that of the wild-type in the temperature range between 40 and 45 °C,[42] whereas the relaxation rate of the fast phase (τ_1) is an order of magnitude faster. To confirm

dx.doi.org/10.1021/jp500774q | J. Phys. Chem. B 2014, 118, 3317−3325

Table 2. Thermodynamic Unfolding Parameters Obtained from CD Measurements

peptide	T_m (°C)	ΔH_m (kcal mol^{-1})	ΔS_m (cal K^{-1} mol^{-1})	ΔC_p (cal K^{-1} mol^{-1})
Trpzip4[a]	70.4	20.2	58.8	374
TZ4-T-CL	67.2 ± 5.2	16.7 ± 1.3	49.1 ± 3.8	337 ± 26
TZ4-T-UC	62.0 ± 3.0	20.2 ± 1.0	60.4 ± 2.9	451 ± 22
TZ4-E-CL	>100	-	-	-
TZ4-E-UL	57.6 ± 2.1	16.5 ± 0.6	50.0 ± 1.8	303 ± 11

[a]From reference 42.

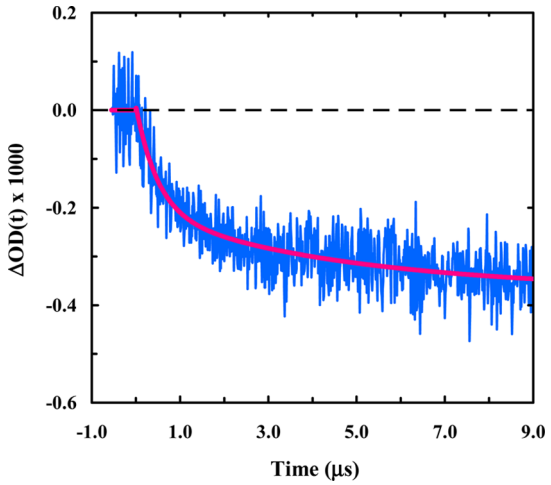

Figure 4. Relaxation kinetics of TZ4-T-CL in response to a T-jump from 28.9 to 39.7 °C. The smooth line represents the best fit of this curve to the following double exponential function: $\Delta OD(t) = A + B_1 \cdot \exp(-t/\tau_1) + B_2 \cdot \exp(-t/\tau_2)$, with $B_1 = 1.75 \times 10^{-4}$, $\tau_1 = 0.50 \pm 0.05$ μs and $B_2 = 1.56 \times 10^{-4}$, $\tau_2 = 4.7 \pm 0.6$ μs.

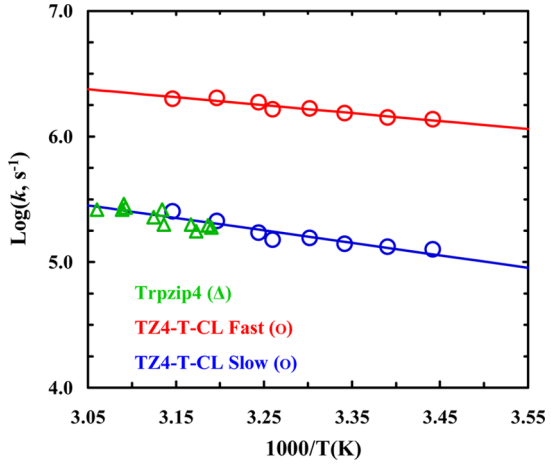

Figure 5. Temperature dependence of the fast and slow relaxation rate constants of TZ4-T-CL, as indicated. The green circles represent the relaxation rate constants of the wild-type Trpzip4 near 40 °C, which are reproduced from ref 42.

that the difference in the relaxation kinetics of TZ4-T-CL and the wild-type originates from the disulfide cross-linker, we also measured the relaxation kinetics of the uncross-linked variant of this peptide (TZ4-T-UL). As shown (Figure 6), the T-jump induced relaxation kinetics of TZ4-T-UL can well be described by a single-exponential function with a rate constant that is slower than that of the wild-type. Further analysis of the relaxation rates, based on a two-state model,[74] indicates that this slowing down predominantly arises from a decrease in the

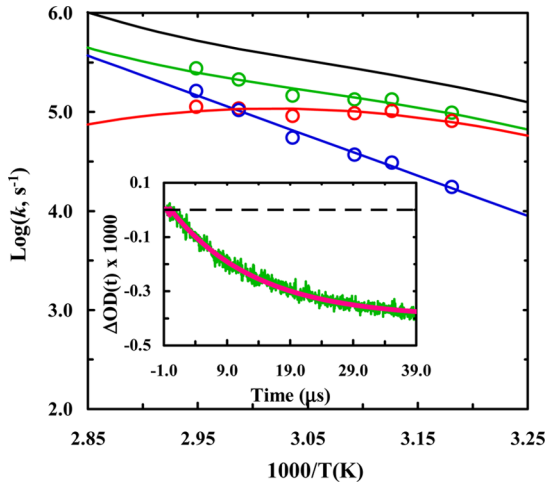

Figure 6. Temperature dependence of the relaxation (green), folding (red) and unfolding (blue) rate constants of TZ4-T-UL. The black smooth line represents the relaxation rate constant of the wild-type Trpzip4, reproduced from ref 42. Shown in the inset is a representative relaxation curve (green) of TZ4-T-UL in response to a T-jump from 33.2 to 41.2 °C, and the smooth line represents the best fit of this curve to a single-exponential function with a relaxation time constant of 13.6 ± 1.4 μs.

folding rate (Figure 6). For example, at 40 °C the folding and unfolding rate constants of TZ4-T-UL are determined to be $(13.3\ \mu s)^{-1}$ and $(66.0\ \mu s)^{-1}$, respectively, compared to $(6.6\ \mu s)^{-1}$ and $(48.4\ \mu s)^{-1}$ of the wild-type. This result is in agreement with the notion that the turn is at least partially, if not completely, formed in the transition state as these cysteine mutations, as shown above (Figure 3), destabilize the native fold. Additionally, the relaxation rate of the slow phase in TZ4-T-CL is at least 2 times faster than that of TZ4-T-UL, thus ruling out the possibility that the double-exponential kinetics observed in TZ4-T-CL could be due to a mixture of oxidized and reduced disulfides.

To further confirm that the double-exponential relaxation behavior observed is unique to TZ4-T-CL, we have also studied a second disulfide Trpzip4 variant, TZ4-E-CL, where the cross-linker is introduced at the termini of the β-hairpin and, hence, is not directly involved with interstrand hydrogen bonding or key side chain interactions. As shown (Figure 7), similar to those observed for the wild-type and TZ4-T-UL, the T-jump induced conformational relaxation kinetics, measured only at high temperatures because of the peptide's high stability (Table 2), are single-exponential. Thus, these results provide further evidence supporting the notion that the disulfide cross-linker in TZ4-T-CL is unique in that it alters the folding mechanism of Trpzip4.

Evidence Suggesting the Population of a Folding TSA in the Unfolded State. The fact that the conformational

dx.doi.org/10.1021/jp500774q | J. Phys. Chem. B 2014, 118, 3317−3325

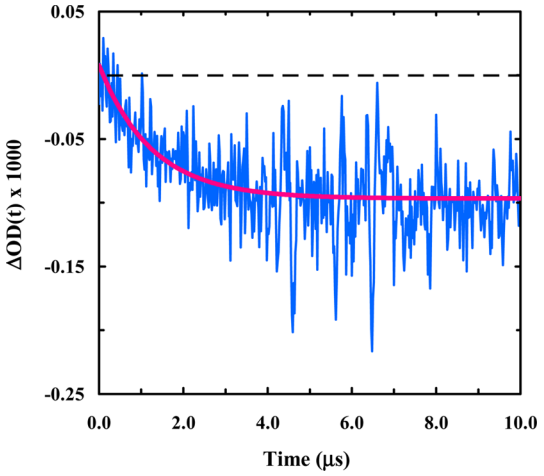

Figure 7. Relaxation kinetics of TZ4-E-CL in response to a *T*-jump from 69.7 to 82.0 °C. The smooth line represents the best fit of this curve to a single-exponential function with a time constant of 1.3 ± 0.5 *μ*s.

relaxation of TZ4-T-CL occurs in a distinctively different manner than that of Trpzip4 wild-type suggests that the cross-linker acts to introduce either an additional folding pathway by forming two distinct unfolded conformational states, as indicated in Figure 1, or an on-pathway folding intermediate (i.e., I in a sequential folding mechanism U → I → F). Distinguishing between these two possibilities is not easy, as both could give rise to double-exponential relaxation kinetics with two drastically different rate constants. However, MD simulations provide evidence indicating the presence of two unfolded populations. As a result, we propose that the folding mechanism follows the cartoon shown in Figure 1, where there are two pathways to the folded state: one with a barrier (i.e., from U_B) similar to the wild-type, and one (i.e., from U_A) with a much smaller barrier or no barrier at all.

The above results support the notion that the disulfide cross-linker in TZ4-T-CL modifies the mechanism of Trpzip4 folding by creating a partially folded, thermodynamically accessible state, U_A, which folds on an ultrafast time scale (~500 ns at 40 °C). In addition, a simple calculation, using the relaxation rate constants of U_A and U_B, suggests that the difference in their folding free energy barrier heights (i.e., $\Delta\Delta G^{\ddagger}$) is about 2.4 k_BT. Considering that U_B has roughly the same relaxation rates as the wild-type and that small proteins typically have a free energy barrier in the range of 2−4 k_BT,[2,75−78] these results suggest that the folding of U_A (Figure 1) proceeds without encountering any significant free energy barriers. In other words, we believe that U_A behaves like a TSA and its folding rate, approximately $(500\ \text{ns})^{-1}$, reports on the dynamics of a fundamental event in *β*-hairpin folding, namely, the process taking the system from the transition state to the folded state.

To provide further evidence supporting the proposed folding mechanism, we carried out free energy calculations on TZ4-T-CL. Specifically, we generated the folding free energy landscape of TZ4-T-CL using MD simulations at 313 K as a function of turn residues, which include Asp7-Lys10, and the residues outside the turn region that are also involved in interstrand hydrogen bonding (referred to as *β* residues). As shown (Figure 8), the simulations clearly indicate that two major unfolded populations are present, with one having a folded turn structure (Figure S2, Supporting Information) and likely corresponding to the proposed U_A state. In addition, there is no apparent barrier between this unfolded state and the folded state, indicative of a downhill folding pathway. The second unfolded population observed in the simulations corresponds to a fully unfolded structure (Figure S3, Supporting Information) with none of the turn and *β*-strand residues being native-like and, thus, is consistent with the proposed U_B state. Unlike the partially unfolded state, folding from this fully unfolded state involves a free energy barrier of ~3.0 k_BT, which agrees well with the value of ~2.4 k_BT calculated from

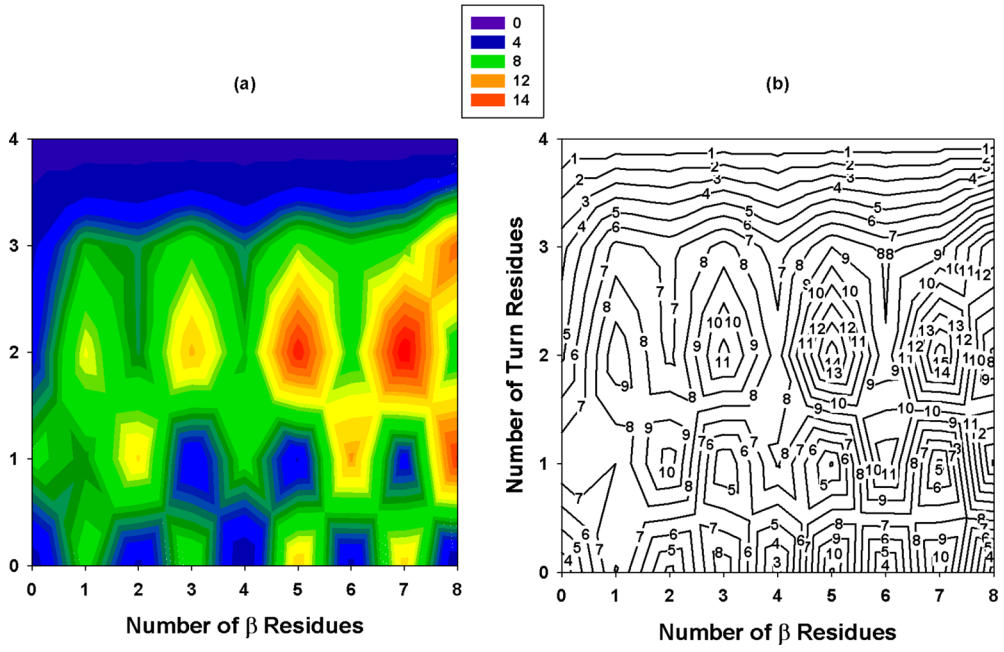

Figure 8. Simulated free energy landscape of TZ4-T-CL presented as function of *β*-strand residues versus the number of turn residues at 313K. The interval between the contour lines is 1 k_BT.

dx.doi.org/10.1021/jp500774q | J. Phys. Chem. B 2014, 118, 3317−3325

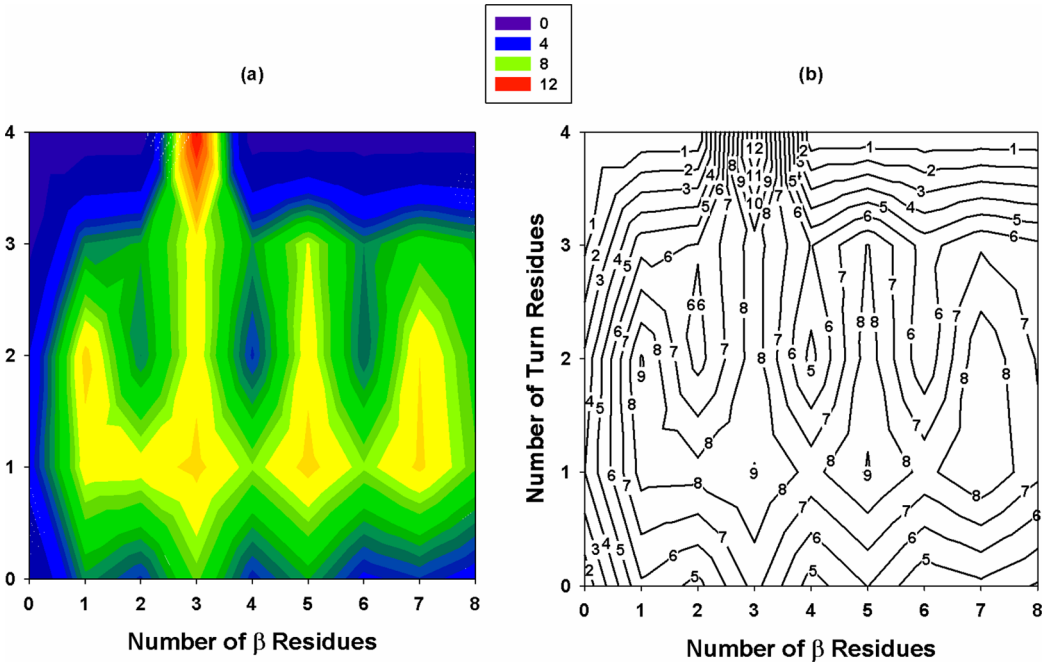

Figure 9. Simulated free energy landscape of Trpzip4 wild-type presented as a function β-strand residues versus the number of turn residues at 313K. The interval between the contour lines is 1 k_BT.

experiments. Similarly, simulations indicate that converting the fully unfolded state to the partially unfolded state also involves a free barrier that amounts to ~3.0 k_BT. For comparison, we also computed the folding free energy landscape of Trpzip4 wild-type. As shown (Figure 9), the folding free energy barrier is ~5.0 k_BT, which is in close range to the barrier height observed for U_B in TZ4-T-CL. However, if folding were assumed to begin from an unfolded state similar to U_A, the free energy barrier is significantly higher, showing that the disulfide cross-linker can indeed play a key role in modulating the folding free energy landscape.

In addition, a recent study by Dyer and co-workers[79] showed that a designed mini-β-hairpin, CLN025, a variant of Chignolin, with a preformed turn in the unfolded state, has a folding rate of $(\sim 100\ \text{ns})^{-1}$ at 40 °C. They attribute this ultrafast rate to an early hydrophobic collapsed structure that results in a free energy landscape with a minimal folding barrier. As a consequence, the folding rate is limited only by local rearrangements required to accommodate native hydrogen bond formation. Since Hamm and co-workers have shown that the rate of hydrogen bond formation occurs on a picosecond time scale,[80] then the difference in the folding rates of CLN025 and TZ4-T-CL (from U_A) most likely reflects the difference in the times required to bring the two chains to their native geometries in these two cases. In other words, the rate of β-hairpin structural evolution, from the transition state, should be limited by the chain diffusion rate or the rate of loop closure and, as a result, the longer folding time of TZ4-T-CL (from U_A) is due to its longer chain length. To provide further support of this notion, we analyzed how the folding rate depends on chain length, using the number of native hydrogen bonds as a proxy. Assuming that the turn is preformed for both CLN025 and TZ4-T-CL (from state U_A), folding then involves propagation of two or four hydrogen bonds, respectively. As shown (Figure 10), the folding time shows a power law dependence on the number of native hydrogen bonds to be propagated and, perhaps more interestingly, the value of the

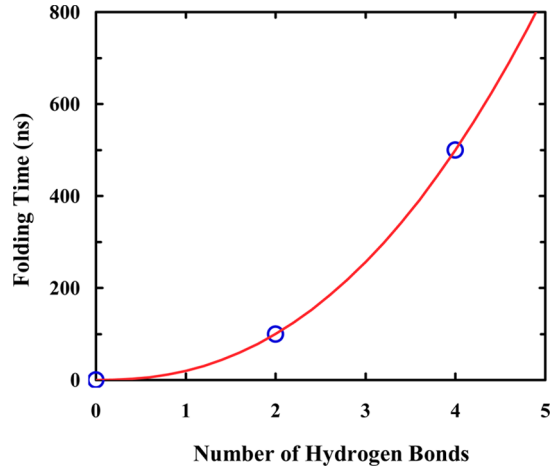

Figure 10. Dependence of the folding time (τ) on the number of native hydrogen bonds (n_H). The smooth line represents the best fit of these points to the following equation: $\tau = \tau_0 n_H^{\alpha}$, with τ_0 = 20 ns and α = 2.3.

exponent (2.3) is almost identical to that (2.4) determined by Makarov and co-workers[81] for end-to-end loop closure time with respect to length for unstructured polymer chains. Not only does this finding provide further evidence indicating that the folding of TZ4-T-CL, when it starts from state U_A, encounters a small, if any, free energy barrier, but it also suggests that the time it takes to form native contacts in a peptide chain in a downhill folding scenario can be estimated by the rate of loop closure. Finally, another line of evidence supporting the aforementioned power law relationship is that the rate of adding an extra β-strand onto a folded three-stranded β-sheet protein, which involves formation of four interstrand hydrogen bonds in a barrierless manner, was also found to be approximately $(500\ \text{ns})^{-1}$ at 40 °C.[82]

dx.doi.org/10.1021/jp500774q | J. Phys. Chem. B 2014, 118, 3317−3325

CONCLUSIONS

The transition state is the hallmark of protein folding dynamics. However, due to its transient nature, taking a snapshot of the folding transition state with sufficient structural resolution is inaccessible by current experimental techniques. Thus, it would be helpful to devise a method that could create stable structural analogues of the transition state. Here, we propose that it is possible to utilize a side chain cross-linker to restrict a particular backbone−backbone hydrogen bond site, thus allowing for the creation of a thermodynamically stable state analogous to the transition state. In a proof-of-principle study, we apply this idea to a small β-hairpin model, Trpzip4, the transition state of which has been shown to involve turn formation. By strategically introducing a disulfide constraint in the turn region that, we believe, would facilitate native turn formation even in the unfolded state, we find that the conformational relaxation kinetics of the disulfide-bond-containing Trpzip4 has two phases, indeed indicative of the presence of an additional state. Further evidence supporting the notion that this cross-linked Trpzip4 has an unfolded state that mimics the folding transition state of the wild-type is that the folding rate of this state, about $(500\ \text{ns})^{-1}$ at 40 °C, is approximately an order of magnitude faster than the wild-type. In addition, a simple analysis of the folding rate obtained from these results reveals that cross-linking the turn induces a free energy barrier decrease of ∼2.4 k_BT. Furthermore, MD simulations performed on the cross-linked Trpzip4 variant also corroborate the notion that two distinct unfolded populations are present: one with a preformed turn that folds via a barrierless pathway, and a second fully unfolded state that encounters a folding free energy barrier similar to that of the wild-type. More interestingly, we find that the time required to propagate a number of native hydrogen bond contacts after the major folding barrier follows a similar length dependence as observed in loop closure kinetics.

ASSOCIATED CONTENT

Supporting Information

Details about global fitting of the CD thermal denaturation curves, 1D ^{1}H NMR spectrum, and representative snapshots from MD simulations. This material is available free of charge via the Internet at http://pubs.acs.org.

AUTHOR INFORMATION

Corresponding Authors

*E-mail: gai@sas.upenn.edu.
*E-mail: gaoyq@pku.edu.cn.

Notes

The authors declare no competing financial interest.

ACKNOWLEDGMENTS

We gratefully acknowledge financial support from the National Institutes of Health (GM-065978 to FG), the Natural Science Foundation of China (21125311 and 21233002 toYQG), and the Ministry of Science and Technology of China (2012CB917304 toYQG). We also thank Dr. George Furst at the University of Pennsylvania for assistance with NMR measurements.

REFERENCES

(1) Bryngelson, J. D.; Onuchic, J. N.; Socci, N. D.; Wolynes, P. G. Funnels, Pathways, and the Energy Landscape of Protein Folding: A Synthesis. *Proteins: Struct., Funct., Bioinf.* **1995**, *21*, 167−195.
(2) Kubelka, J.; Hofrichter, J.; Eaton, W. A. The Protein Folding 'Speed Limit'. *Curr. Opin. Struct. Biol.* **2004**, *14*, 76−88.
(3) Dill, K. A.; Ozkan, S. B.; Shell, M. S.; Weikl, T. R. The Protein Folding Problem. *Annu. Rev. Biophys.* **2008**, *37*, 289−316.
(4) Royer, C. A. The Nature of the Transition State Ensemble and the Mechanisms of Protein Folding: A Review. *Arch. Biochem. Biophys.* **2008**, *469*, 34−45.
(5) Moran, L. B.; Schneider, J. P.; Kentsis, A.; Reddy, G. A.; Sosnick, T. R. Transition State Heterogeneity in GCN4 Coiled Coil Folding Studied by using Multisite Mutations and Crosslinking. *Proc. Natl. Acad. Sci. U. S. A.* **1999**, *96*, 10699−10704.
(6) Krantz, B. A.; Sosnick, T. R. Engineered Metal Binding Sites Map the Heterogeneous Folding Landscape of a Coiled Coil. *Nat. Struct. Biol.* **2001**, *8*, 1042−1047.
(7) Fersht, A. R.; Daggett, V. Protein Folding and Unfolding at Atomic Resolution. *Cell* **2002**, *108*, 573−582.
(8) Geierhaas, C. D.; Salvatella, X.; Clarke, J.; Vendruscolo, M. Characterisation of Transition State Structures for Protein Folding using 'High', 'Medium' and 'Low' Φ-Values. *Protein Eng., Des. Sel.* **2008**, *21*, 215−222.
(9) Matouschek, A.; Kellis, J. T.; Serrano, L.; Fersht, A. R. Mapping the Transition-State and Pathway of Protein Folding by Protein Engineering. *Nature* **1989**, *340*, 122−126.
(10) Fersht, A. R. Nucleation Mechanisms in Protein Folding. *Curr. Opin. Struct. Biol.* **1997**, *7*, 3−9.
(11) Fersht, A. R.; Sato, S. Φ-Value Analysis and the Nature of Protein-Folding Transition States. *Proc. Natl. Acad. Sci. U. S. A.* **2004**, *101*, 7976−7981.
(12) Pauling, L. Molecular Architecture and Biological Reactions. *Chem. Eng. News* **1946**, *24*, 1375−1377.
(13) Wolfende., R. Transition State Analogues for Enzyme Catalysis. *Nature* **1969**, *223*, 704−705.
(14) Wolfende., R. Analog Approaches to the Structure of the Transition-State in Enzyme Reactions. *Acc. Chem. Res.* **1972**, *5*, 10−18.
(15) Schramm, V. L. Transition States, Analogues, and Drug Development. *ACS Chem. Biol.* **2013**, *8*, 71−81.
(16) Fedorov, A.; Shi, W.; Kicska, G.; Fedorov, E.; Tyler, P. C.; Furneaux, R. H.; Hanson, J. C.; Gainsford, G. J.; Larese, J. Z.; Schramm, V. L.; Almo, S. C. Transition State Structure of Purine Nucleoside Phosphorylase and Principles of Atomic Motion in Enzymatic Catalysis. *Biochemistry* **2001**, *40*, 853−860.
(17) Schramm, V. L. Enzymatic Transition State Theory and Transition State Analogue Design. *J. Biol. Chem.* **2007**, *282*, 28297−28300.
(18) Klimov, D. K.; Thirumalai, D. Mechanisms and Kinetics of β-Hairpin Formation. *Proc. Natl. Acad. Sci. U. S. A.* **2000**, *97*, 2544−2549.
(19) Kobayashi, N.; Honda, S.; Yoshii, H.; Munekata, E. Role of Side-Chains in the Cooperative β-Hairpin Folding of the Short C−Terminal Fragment Derived from Streptococcal Protein G. *Biochemistry* **2000**, *39*, 6564−6571.
(20) Espinosa, J. F.; Syud, F. A.; Gellman, S. H. Analysis of the Factors that Stabilize a Designed Two-Stranded Antiparallel β-Sheet. *Protein Sci.* **2002**, *11*, 1492−1505.
(21) Maness, S. J.; Franzen, S.; Gibbs, A. C.; Causgrove, T. P.; Dyer, R. B. Nanosecond Temperature Jump Relaxation Dynamics of Cyclic β-Hairpin Peptides. *Biophys. J.* **2003**, *84*, 3874−3882.
(22) Baumketner, A.; Shea, J. E. The Thermodynamics of Folding of a β Hairpin Peptide Probed Through Replica Exchange Molecular Dynamics Simulations. *Theor. Chem. Acc.* **2006**, *116*, 262−273.
(23) Petrovich, M.; Jonsson, A. L.; Ferguson, N.; Daggett, V.; Fersht, A. R. Φ-Analysis at the Experimental Limits: Mechanism of β-Hairpin Formation. *J. Mol. Biol.* **2006**, *360*, 865−881.
(24) Best, R. B.; Mittal, J. Microscopic Events in β-Hairpin Folding from Alternative Unfolded Ensembles. *Proc. Natl. Acad. Sci. U. S. A.* **2011**, *108*, 11087−11092.

(25) Xu, Y.; Du, D.; Oyola, R. Infrared Study of the Stability and Folding Kinetics of a Series of β-Hairpin Peptides with a Common NPDG Turn. *J. Phys. Chem. B* **2011**, *115*, 15332−15338.
(26) Santiveri, C. M.; Leon, E.; Rico, M.; Jimenez, M. A. Context-Dependence of the Contiribution of Disulfide Bonds to β-Hairpin Stability. *Chem.—Eur. J.* **2008**, *14*, 488−499.
(27) Carulla, N.; Woodward, C.; Barany, G. Synthesis and Characterization of a β-Hairpin Peptide that Represents a 'Core Module' of Bovine Pancreatic Trypsin Inhibitor (BPTI). *Biochemistry* **2000**, *39*, 7927−7937.
(28) Russell, S. J.; Blandl, T.; Skelton, N. J.; Cochran, A. G. Stability of Cyclic β-Hairpins: Asymmetric Contributions from Side Chains of a Hydrogen-Bonded Cross-Strand Residue Pair. *J. Am. Chem. Soc.* **2003**, *125*, 388−395.
(29) Du, D. G.; Gai, F. Understanding the Folding Mechanism of an α-Helical Hairpin. *Biochemistry* **2006**, *45*, 13131−13139.
(30) Mirassou, Y.; Santiveri, C. M.; Pérez de Vega, M. J.; González-Muñiz, R.; Jiménez, M. A. Disulfide Bonds versus Trp···Trp Pairs in Irregular β-Hairpins: NMR Structure of Vammin Loop 3-Derived Peptides as a Case Study. *ChemBioChem* **2009**, *10*, 902−910.
(31) Jo, H.; Meinhardt, N.; Wu, Y. B.; Kulkarni, S.; Hu, X. Z.; Low, K. E.; Davies, P. L.; DeGrado, W. F.; Greenbaum, D. C. Development of α-Helical Calpain Probes by Mimicking a Natural Protein−Protein Interaction. *J. Am. Chem. Soc.* **2012**, *134*, 17704−17713.
(32) Ihalainen, J. A.; Paoli, B.; Muff, S.; Backus, E. H. G.; Bredenbeck, J.; Woolley, G. A.; Caflisch, A.; Hamm, P. α-Helix Folding in the Presence of Structural Constraints. *Proc. Natl. Acad. Sci. U. S. A.* **2008**, *105*, 9588−9593.
(33) Tucker, M. J.; Courter, J. R.; Chen, J. X.; Atasoylu, O.; Smith, A. B.; Hochstrasser, R. M. Tetrazine Phototriggers: Probes for Peptide Dynamics. *Angew. Chem., Int. Ed.* **2010**, *49*, 3612−3616.
(34) Clarke, J.; Fersht, A. R. Engineered Disulfide Bonds as Probes of the Folding Pathway of Barnase: Increasing the Stability of Proteins Against the Rate of Denaturation. *Biochemistry* **1993**, *32*, 4322−4329.
(35) Grantcharova, V. P.; Riddle, D. S.; Baker, D. Long-range order in the src SH3 folding transition state. *Proc. Natl. Acad. Sci. U.S.A.* **2000**, *97*, 7084−7089.
(36) Wang, T.; Lau, W. L.; DeGrado, W. F.; Gai, F. T-Jump Infrared Study of the Folding Mechanism of Coiled-Coil GCN4-p1. *Biophys. J.* **2005**, *89*, 4180−4187.
(37) Shandiz, A. T.; Capraro, B. R.; Sosnick, T. R. Intramolecular Cross-Linking Evaluated as a Structural Probe of the Protein Folding Transition State. *Biochemistry* **2007**, *46*, 13711−13719.
(38) Chung, H. S.; Shandiz, A.; Sosnick, T. R.; Tokmakoff, A. Probing the Folding Transition State of Ubiquitin Mutants by Temperature-Jump-Induced Downhill Unfolding. *Biochemistry* **2008**, *47*, 13870−13877.
(39) Munoz, V.; Thompson, P. A.; Hofrichter, J.; Eaton, W. A. Folding Dynamics and Mechanism of β-Hairpin Formation. *Nature* **1997**, *390*, 196−199.
(40) Chen, R. P.-Y.; Huang, J. J.-T.; Chen, H.-L.; Jan, H.; Velusamy, M.; Lee, C.-T.; Fann, W.; Larsen, R. W.; Chan, S. I. Measuring the Refolding of β-Sheets with Different Turn Sequences on a Nanosecond Time Scale. *Proc. Natl. Acad. Sci. U. S. A.* **2004**, *101*, 7305−7310.
(41) Dyer, R. B.; Maness, S. J.; Peterson, E. S.; Franzen, S.; Fesinmeyer, R. M.; Andersen, N. H. The Mechanism of β-Hairpin Formation. *Biochemistry* **2004**, *43*, 11560−11566.
(42) Du, D.; Zhu, Y.; Huang, C. Y.; Gai, F. Understanding the Key Factors that Control the Rate of β-Hairpin Folding. *Proc. Natl. Acad. Sci. U. S. A.* **2004**, *101*, 15915−15920.
(43) Yang, W. Y.; Pitera, J. W.; Swope, W. C.; Gruebele, M. Heterogeneous Folding of the Trpzip Hairpin: Full Atom Simulation and Experiment. *J. Mol. Biol.* **2004**, *336*, 241−251.
(44) Du, D.; Tucker, M. J.; Gai, F. Understanding the Mechanism of β-Hairpin Folding via Φ-Value Analysis. *Biochemistry* **2006**, *45*, 2668−2678.
(45) Pitera, J. W.; Haque, I.; Swope, W. C. Absence of Reptation in the High-Temperature Folding of the Trpzip2 β-Hairpin Peptide. *J. Chem. Phys.* **2006**, *124*, 141102.
(46) Zhang, J.; Qin, M.; Wang, W. Folding Mechanism of β-Hairpins Studied by Replica Exchange Molecular Simulations. *Proteins: Struct., Funct., Bioinf.* **2006**, *62*, 672−685.
(47) Narayanan, R.; Pelakh, L.; Hagen, S. J. Solvent Friction Changes the Folding Pathway of the Tryptophan Zipper TZ2. *J. Mol. Biol.* **2009**, *390*, 538−546.
(48) Roy, S.; Jansen, T. L. C.; Knoester, J. Structural Classification of the Amide I Sites of a β-Hairpin with Isotope Label 2DIR Spectroscopy. *Phys. Chem. Chem. Phys.* **2010**, *12*, 9347−9357.
(49) Smith, A. W.; Lessing, J.; Ganim, Z.; Peng, C. S.; Tokmakoff, A.; Roy, S.; Jansen, T. L. C.; Knoester, J. Melting of a β-Hairpin Peptide Using Isotope-Edited 2D IR Spectroscopy and Simulations. *J. Phys. Chem. B* **2010**, *114*, 10913−10924.
(50) Huang, J. J. T.; Larsen, R. W.; Chan, S. I. The Interplay of Turn Formation and Hydrophobic Interactions on the Early Kinetic Events in Protein Folding. *Chem. Commun.* **2012**, *48*, 487−497.
(51) Deeg, A. A.; Rampp, M. S.; Popp, A.; Pilles, B. M.; Schrader, T. E.; Moroder, L.; Hauser, K.; Zinth, W. Isomerization- and Temperature-Jump-Induced Dynamics of a Photoswitchable β-Hairpin. *Chem.—Eur. J.* **2013**, *20*, 694−703.
(52) Serrano, A. L.; Waegele, M. M.; Gai, F. Spectroscopic Studies of Protein Folding: Linear and Nonlinear Methods. *Protein Sci.* **2012**, *21*, 157−170.
(53) Tam, J. P.; Wu, C. R.; Liu, W.; Zhang, J. W. Disulfide Bond Formation in Peptides by Dimethyl Sulfoxide. Scope and Applications. *J. Am. Chem. Soc.* **1991**, *113*, 6657−6662.
(54) Culik, R. M.; Serrano, A. L.; Bunagan, M. R.; Gai, F. Achieving Secondary Structural Resolution in Kinetic Measurements of Protein Folding: A Case Study of the Folding Mechanism of Trp-Cage. *Angew. Chem., Int. Ed.* **2011**, *50*, 10884−10887.
(55) Cornell, W. D.; Cieplak, P.; Bayly, C. I.; Gould, I. R.; Merz, K. M.; Ferguson, D. M.; Spellmeyer, D. C.; Fox, T.; Caldwell, J. W.; Kollman, P. A. A 2nd Generation Force-Field for the Simulation of Proteins, Nucleic-Acids, and Organic-Molecules. *J. Am. Chem. Soc.* **1995**, *117*, 5179−5197.
(56) Onufriev, A.; Bashford, D.; Case, D. A. Exploring Protein Native States and Large-Scale Conformational Changes with a Modified Generalized Born Model. *Proteins* **2004**, *55*, 383−394.
(57) Ryckaert, J. P.; Ciccotti, G.; Berendsen, H. J. C. Numerical-Integration of Cartesian Equations of Motion of a System with Constraints - Molecular-Dynamics of N-Alkanes. *J. Comput. Phys.* **1977**, *23*, 327−341.
(58) Gao, Y. Q. An Integrate-Over-Temperature Approach for Enhanced Sampling. *J. Chem. Phys.* **2008**, *128*, 064105.
(59) Shao, Q. A.; Gao, Y. Q. Temperature Dependence of Hydrogen-Bond Stability in β-Hairpin Structures. *J. Chem. Theory Comput.* **2010**, *6*, 3750−3760.
(60) Yang, L. J.; Shao, Q.; Gao, Y. Q. Enhanced Sampling Method in Molecular Simulations. *Prog. Chem.* **2012**, *24*, 1199−1213.
(61) Olsen, K. A.; Fesinmeyer, R. M.; Stewart, J. M.; Andersen, N. H. Hairpin Folding Rates Reflect Mutations Within and Remote from the Turn Region. *Proc. Natl. Acad. Sci. U. S. A.* **2005**, *102*, 15483−15487.
(62) Streicher, W. W.; Makhatadze, G. I. Calorimetric Evidence for a Two-State Unfolding of the β-Hairpin Peptide Trpzip4. *J. Am. Chem. Soc.* **2006**, *128*, 30−31.
(63) Shao, Q.; Wei, H.; Gao, Y. Q. Effects of Turn Stability and Side-Chain Hydrophobicity on the Folding of β-Structures. *J. Mol. Biol.* **2010**, *402*, 595−609.
(64) Hwang, S.; Hilty, C. Folding of a Tryptophan Zipper Peptide Investigated on the Basis of the Nuclear Overhauser Effect and Thermal Denaturation. *J. Phys. Chem. B* **2011**, *115*, 15355−15361.
(65) Juraszek, J.; Vreede, J.; Bolhuis, P. G. Transition Path Sampling of Protein Conformational Changes. *Chem. Phys.* **2012**, *396*, 30−44.
(66) Liao, C. Y.; Zhou, J. Replica Exchange Molecular Dynamics Simulations on the Folding of Trpzip4 β-Hairpin. *Acta Chim. Sin.* **2013**, *71*, 593−601.

(67) Cochran, A. G.; Skelton, N. J.; Starovasnik, M. A. Tryptophan Zippers: Stable, Monomeric β-Hairpins. *Proc. Natl. Acad. Sci. U. S. A.* **2001**, *98*, 5578−5583.
(68) Wu, L.; McElheny, D.; Takekiyo, T.; Keiderling, T. A. Geometry and Efficacy of Cross-Strand Trp/Trp, Trp/Tyr, and Tyr/Tyr Aromatic Interaction in a β-Hairpin Peptide. *Biochemistry* **2010**, *49*, 4705−4714.
(69) Grishina, I. B.; Woody, R. W. Contributions of Tryptophan Side Chains to the Circular Dichroism of Globular Proteins: Exciton Couplets and Coupled Oscillators. *Faraday Discuss.* **1994**, *99*, 245−262.
(70) Guvench, O.; Brooks, C. L. Tryptophan Side Chain Electrostatic Interactions Determine Edge-to-Face vs Parallel-Displaced Tryptophan Side Chain Geometries in the Designed β-Hairpin "trpzip2". *J. Am. Chem. Soc.* **2005**, *127*, 4668−4674.
(71) Wu, L.; McElheny, D.; Huang, R.; Keiderling, T. A. Role of Tryptophan−Tryptophan Interactions in Trpzip β-Hairpin Formation, Structure, and Stability. *Biochemistry* **2009**, *48*, 10362−10371.
(72) Abkevich, V. I.; Shakhnovich, E. I. What can Disulfide Bonds Tell us About Protein Energetics, Function and Folding: Simulations and Bioninformatics Analysis. *J. Mol. Biol.* **2000**, *300*, 975−985.
(73) Fesinmeyer, R. M.; Hudson, F. M.; Andersen, N. H. Enhanced Hairpin Stability through Loop Design: The Case of the Protein G B1 Domain Hairpin. *J. Am. Chem. Soc.* **2004**, *126*, 7238−7243.
(74) Markiewicz, B. N.; Jo, H.; Culik, R. M.; DeGrado, W. F.; Gai, F. Assessment of local friction in protein folding dynamics using a helix cross-linker. *J. Phys. Chem. B* **2013**, *117*, 14688−14696.
(75) Yang, W. Y.; Gruebele, M. Folding at the Speed Limit. *Nature* **2003**, *423*, 193−197.
(76) Snow, C. D.; Qiu, L.; Du, D.; Gai, F.; Hagen, S. J.; Pande, V. S. Trp Zipper Folding Kinetics by Molecular Dynamics and Temperature-Jump Spectroscopy. *Proc. Natl. Acad. Sci. U. S. A.* **2004**, *101*, 4077−4082.
(77) Dyer, R. B. Ultrafast and Downhill Protein Folding. *Curr. Opin. Struct. Biol.* **2007**, *17*, 38−47.
(78) Munoz, V.; Sadqi, M.; Naganathan, A. N.; de Sancho, D. Exploiting the Downhill Folding Regime via Experiment. *HFSP J.* **2008**, *2*, 342−353.
(79) Davis, C. M.; Xiao, S.; Raleigh, D. P.; Dyer, R. B. Raising the Speed Limit for β-Hairpin Formation. *J. Am. Chem. Soc.* **2012**, *134*, 14476−14482.
(80) Kolano, C.; Helbing, J.; Kozinski, M.; Sander, W.; Hamm, P. Watching Hydrogen-Bond Dynamics in a β-Turn by Transient Two-Dimensional Infrared Spectroscopy. *Nature* **2006**, *444*, 469−472.
(81) Cheng, R. R.; Uzawa, T.; Plaxco, K. W.; Makarov, D. E. Universality in the Timescales of Internal Loop Formation in Unfolded Proteins and Single-Stranded Oligonucleotides. *Biophys. J.* **2010**, *99*, 3959−3968.
(82) Xu, Y.; Bunagan, M. R.; Tang, J.; Gai, F. Probing the Kinetic Cooperativity of β-Sheet Folding Perpendicular to the Strand Direction. *Biochemistry* **2008**, *47*, 2064−2070.